UNITED NATIONS UNIVERSITY
UNU-GTP
Geothermal Training Programme

Orkustofnun, Grensasvegur 9,
IS-108 Reykjavik, Iceland

Reports 2018
Number 24

DESIGN OF A HYPOTHETICAL DDP-WELL IN TIBET YANGYI, CHINA

Ren Xiaoqing
Sinopec Green Energy Geothermal Development Co., Ltd.
Construction Building, Zhonghua West Road, Qindu District
Xianyang City
Shaanxi Province
CHINA
renxiaoqing.xxsy@sinopec.com

ABSTRACT

This paper first introduces the ins and outs of IDDP, the main achievements and the basic geological conditions of the Tibet Yangyi area in China. Secondly, we combine existing well data, the fitting and analyzing deep temperature and pressure conditions, together with IDDP geothermal well design experience, to apply the minimum casing depth design method to calculate the depth of each casing of the geothermal well in the Yangyi area. Through calculation and analysis of each main pressure, the main technical parameters of the casings are obtained. The research ideas and methods presented in this project report have a certain reference for the development of supercritical geothermal resources in the Yangyi area of Tibet, China.

1. INTRODUCTION

The Iceland Deep Drilling Project (IDDP) has received international attention since its inception at the beginning of this century. The difference between this project and conventional geothermal development is that it focuses on supercritical geothermal fluids, i.e. with temperatures above 374.15°C and pressures exceeding 22.12 MPa. After eight years of preparation, feasibility demonstration and repeated discussion, the project partners successfully drilled the IDDP-1 well (Fridleifsson and Richter, 2010). The well hit magma before the planned completion depth could be reached. The mining of such high-temperature and high-pressure geothermal fluids makes higher demands on the design of the wellbore structure of geothermal wells. The minimum depth design of traditional geothermal well casings only considers boiling point with depth (BPD) and fracture pressure. In the IDDP project, the casing minimum depth design did not only considers BPD but also the relationship between cold water pressure and depth as well as the relationship between heavy mud pressure and depth in the wellbore. Additionally, the design can be further refined and revised based on accumulated experience.

The Tibet Yangyi geothermal field is located in the Qinghai-Tibet Plateau, China, where the Indian plate collides with the Eurasian plate and continues to lift the Qinghai-Tibet Plateau. The violent plate movement causes earthquake activity and has also created the Tibet Autonomous Region, especially the unique geothermal resources in the Yangyi area. At the end of 2016, 15 geothermal wells had been drilled in the Yangyi area. The deepest well is 1500 m deep, the temperatures are 104-207°C, while the

flow rate is 32-373 m^3/h. Based on this information, geothermal power generation potential has been estimated to be 30 MW. High-temperature geothermal resources have been found in relatively shallow depths in the area. Deep formation temperature and pressures are still widely unknown.

2. THE IDDP PROJECT

2.1 The historical development of IDDP

The IDDP project was established in 2000 and was originally initiated and formed by three Icelandic energy companies, including Hitaveita Sudurnesja (now HS Orka, hf) (HS), Landsvirkjun (LV) and Orkuveita Reykjavíkur (OR), as well as Orkustofnun (OS), the National Energy Authority of Iceland. The basic concept of IDDP was presented at the World Geothermal Congress in Japan which was held in Japan (Fridleifsson and Albertsson, 2000). An overview of key events is shown in Table 1.

TABLE 1: IDDP project development process (Fridleifsson, 2017)

Year	Event
2000	IDDP established by Icelandic energy consortium
2003	A feasibility report completed, supported by ICDP and US NSF for science coring and science.
2004-2006	Well RN-17 at Reykjanes "well of opportunity" for IDDP, collapsed during flow test, only 3 km deep.
2008-2009	Well IDDP-1 drilled at KRAFLA – hit magma at 2.1 km (>900°C) – the hottest production well in the world with super-heated steam at 452°C and 140 bar, enthalpy 3200 kJ/kg, power capacity up to 36 MWe.
2016-2017	Deepening of the 2.5 km deep "well of opportunity" (RN-15) to 4,650 m – as IDDP-2. Drilling began 11th August 2016 and was completed at 4650 m depth 25th January 2017. Funded by HS Orka, Statoil and the IDDP consortium with additional support from DEEPEGS – EU supported a 4-year project. Coring funds from ICDP and NSF used for all IDDP coring. Supercritical conditions measured at ~4,500 m depth 3rd January 2017 during drilling, 426°C and 340 bar.

The IDDP project is a research project that seeks to improve the efficiency and economics of geothermal systems by utilizing deep unconventional geothermal resources. According to Thórhallsson et al. (2010), the goal was to:

1) Drill 4-5 km deep wells in different high-temperature areas in Iceland;
2) Search for geothermal fluids under supercritical conditions, which means that the temperature of pure water exceeds 374.15°C and 22.12 MPa, while the temperature of seawater exceeds 406°C and 29.8 MPa;
3) Investigate the resource potential of 400-600°C and superheated fluids from 3.5-5 km depth. At this depth, the temperature and pressure exceed the critical point of 374.15°C and 22.12 MPa and only a single-phase fluid exists.

Since its inception, the IDDP consortium has carried out extensive international cooperation and scientists from at least 15 countries have contributed to the smooth implementation of the project by attending seminars or participating in related research and publishing papers. Since 2005, the ICDP (International Continental Scientific Drilling Program) and the NSF (National Science Foundation of USA) have been greatly supporting the project. Furthermore, Alcoa (2006-2012) and Statoil (2008-2011) also participated in the implementation of the IDDP-1 project by providing capital or technology (Fridleifsson et al., 2015).

At the start-up meeting, it was emphasized that the IDDP project would offer the scientific community unique opportunities to:

a) Study and sample fluids at supercritical conditions; and
b) Investigate volcanic rocks and fluid circulation in the Mid-Atlantic ridge.

There has never been a chance to directly observe the environment of a high-temperature geothermal system. The Drilling Assessment team conducted five different evaluations of the target. In the end, it was agreed that the best option was to drill a standard production well with a depth of 3.5 km and then use the hybrid-rotary coring technique to continuously drill another 1-1.5 km. From the perspective of earth science and environmental science, the Geological Science Group has developed standards for selecting well conditions. In the end, three geothermal fields were selected, namely Reykjanes, Hengill and Krafla. The have high potential to be supercritical reservoirs with permeability present (Fridleifsson and Richter, 2010).

The IDDP project team submitted a proposal for the workshop to the International Continental Scientific Drilling Program (ICDP) and the Icelandic IDDP energy consortium developed guidelines for a feasibility study of the IDDP concept. Subsequently, three advisory groups were formed, one on the GeoSciences (GS-group), another on the Drilling Technology (DT-group) and the third on a Pilot Plant. The three groups of consultants were from energy companies and consulting companies. Their main task was to evaluate the IDDP concept. At the kick-off meeting, experts from Iceland met with foreign experts and established the basis for future cooperation. A series of review conferences and academic conferences on IDDP have been arranged since and are listed in Table 2.

TABLE 2: List of IDDP planning workshops and organizational meetings (Fridleifsson et al., 2010a)

1. Start-up June 2001	June 2001
2. Drilling technology	March 2002
3. Science programme	October 2003
4. Site selection	June 2004
5. Crisis	March 2006
6. Site selection	March 2007
7. Kick-off meeting	March 2009
8. Fluid handling	September 2009

2.2 Breakthrough results achieved by IDDP

The three selected IDDP well locations represent different tectonic development stages of the Mid-Atlantic Ridge. The Reykjanes site, a direct on-land continuation of the submerged Reykjanes Ridge, represents an immature stage of rifting with a sheeted dike complex as heat source. Here, the fluid extracted from the 2 km deep geothermal well is heated seawater. In the Hengill geothermal area, the relatively young central volcano is the heat source for thermal reservoir and atmospheric precipitation constitutes a source of fluid recharge. The Krafla high-temperature geothermal field is located in the caldera of an active and mature central volcanic complex. Figure 1 shows the locations of the three geothermal fields.

2.2.1 The IDDP-1 well

IDDP-1 well is located in Krafla in the north-eastern part of Iceland. The well was drilled in 2009 and hit magma of rhyolite composition. The temperature exceeded 900°C, so the drilling had to be stopped at 2.1 km depth. The project mines a thermal contact zone with magma intrusion where the temperature is greater than 500°C. The well was completed with a cemented 9 ⅝" sacrificial casing to 1950 m depth inside a 13 ⅝" production casing to the same depth. A 9 ⅝" slotted liner reaches from 1,950 m to 2,072 m depth, while underneath the well is barefoot with 12 ¼" diameter down to 2,096 m depth. Table 3 lists the design parameters of the IDDP-1 well and Figure 2 shows the well design. A drawing of well IDDP-1 is shown in Figure 3.

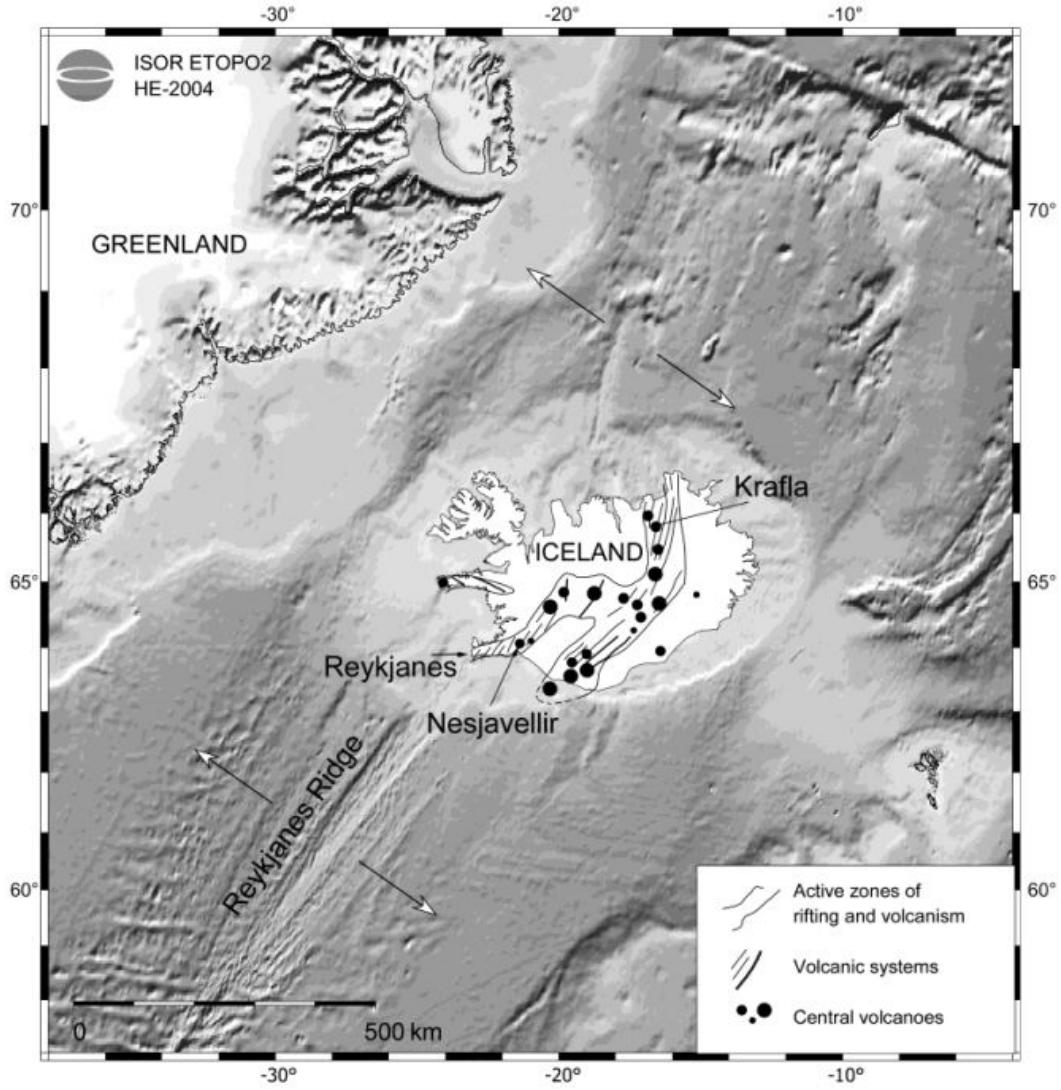

FIGURE 1: The location of Reykjanes, Hengill and Krafla volcanic systems (Fridleifsson et al., 2011; 2015)

TABLE 3: Casing design of IDDP-1 (Hólmgeirsson et al., 2010)

Casing	Drilling procedures
Surface casing	To -100 m - 32”× ½” X56 welded. Wellbore drilled with 26” roller cone bit and 36" under-reamer. Rotary drilled.
Intermediate casing I	To -300 m - 24 ½” 162 lb/ft K55, Tenaris/Hydril 563 threads. Wellbore drilled with 26 ½” roller cone bit. Rotary mud-drilled.
Intermediate casing II	To -800 m - 18 ⅝” 114 lb/ft K55 BTC. Wellbore drilled with 23” roller cone bit. Rotary mud-drilled.
Anchor casing	To -2400 m not incl. top 300 m, 13 ⅝” 88.2 lb/ft T95 Tenaris/Hydril 563 threads and from -300 m to -2400 m 13 ⅜” 72 lb/ft K55 Tenaris/Hydril 563 threads. Wellbore drilled with 16 ½” roller cone bit. Drilled with a mud and a mud motor.
Production casing	To -3500 m - 9 ⅝” 53,5 lb/ft K55 Tenaris/Hydril 563 threads. Wellbore drilled with 12 1/4” roller cone bit. Rotary drilled.
Slotted liner	To -4500 m - 7” 26 lb/ft K55 BTC. Wellbore drilled with 8 ½” roller cone bit. Rotary drilled.

During the geothermal well tests in the next two years, the IDDP wellhead temperature reached 450°C while the wellhead pressure reached 40-140 bar, and superheated dry steam was ejected. After a series of tests, the IDDP-1 well has a production capacity of 36 MWe in accordance with the design of the turbine system. This is a breakthrough in the development of technical capabilities to produce from magmatic reservoirs.

The IDDP project has facilitated major progress in drilling technology which are:

i. The IDDP project managed to drill into molten rock at >900°C and get out of it;
ii. It produced high permeability by hydro fracking the contact aureole rocks with cold drilling fluid;
iii. It managed to insert a protective casing (sacrificial casing), to cement it, and to insert a liner;
iv. It produced superheated dry steam from the contact aureole at world record temperature for a geothermal well;
v. It showed that hostile fluid chemistry could safely be dealt with by steam treatment, enabling the steam to be channelled directly into conventional steam turbines; and finally
vi. It proved beyond reasonable doubt that the world's first Magma-EGS system had been created, confirmed by an injection tracer test after the discharge tests.

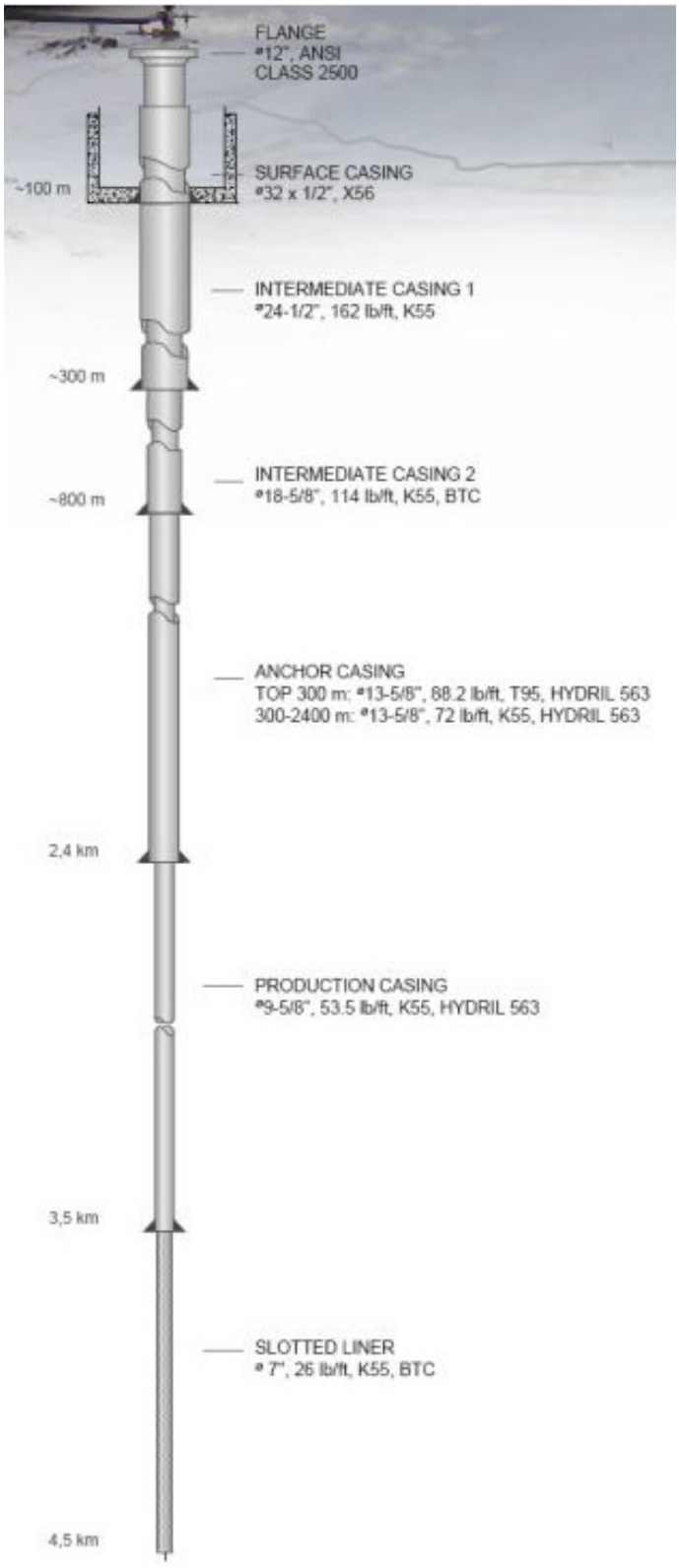

FIGURE 2: Well design of IDDP-1
(Thórhallsson et al., 2010b)

While it would probably be more economical to use the steam directly from a well like IDDP-1 in superheated form, the process could evidently be reversed by using such wells for injection in an attempt to enhance the performance of the conventional geothermal system above. The IDDP-1 well had to be cooled down rather abruptly in 2012 due to valve failure and the pilot studies and flow test terminated. Many technical hurdles were met during drilling and the subsequent flow test of the IDDP-1 well and the lessons learned so far are very valuable for the continuation of the IDDP R&D program (Fridleifsson et al., 2015).

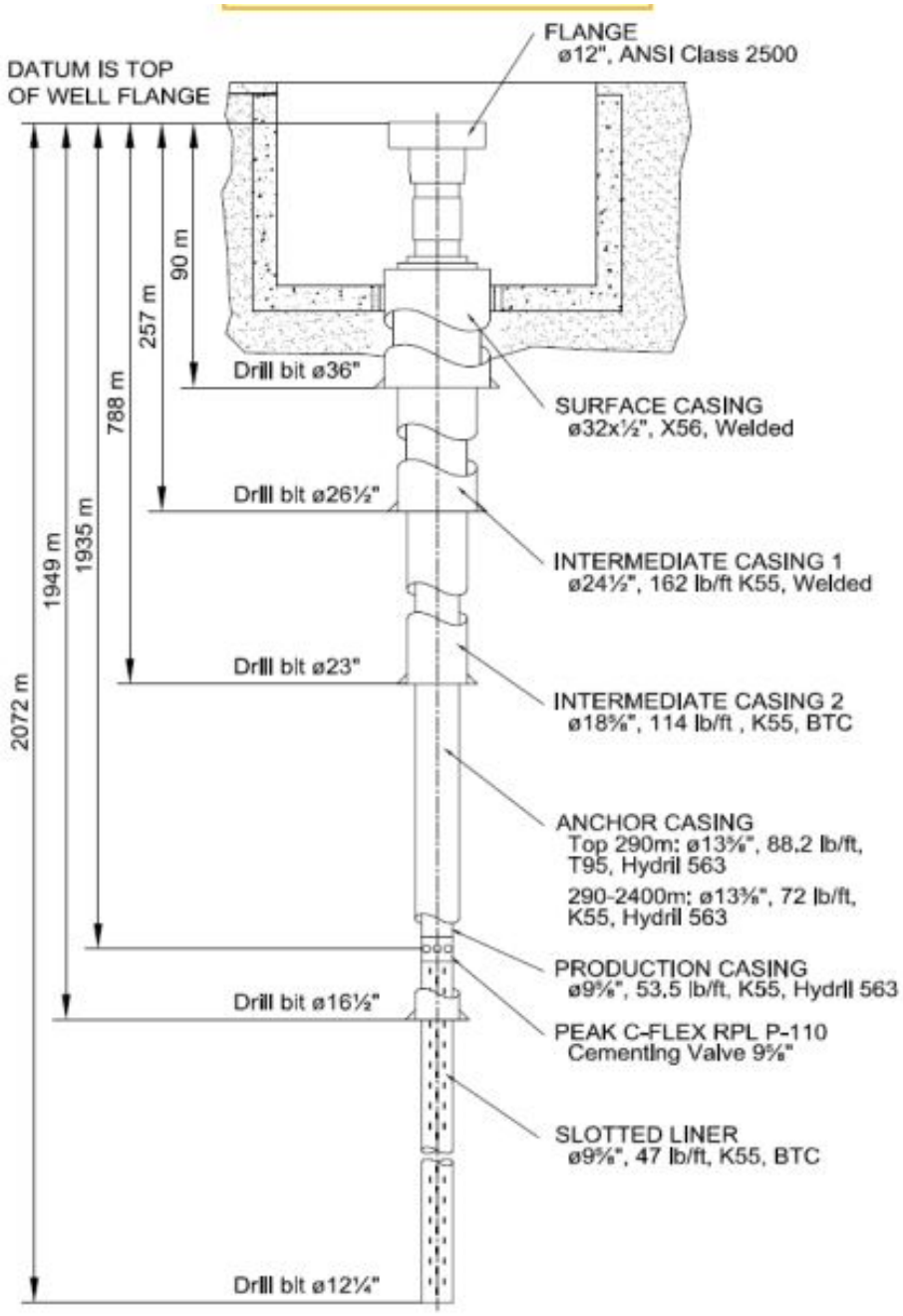

FIGURE 3: Drawing of well IDDP-1 as built (Fridleifsson et al., 2010)

2.2.2 The IDDP-2 well

Numerous casing design options where looked into before settling on the final design for the IDDP-2 well. The IDDP-2 design shown in Figure 4 had to have fewer casings down to 5000 m depth than IDDP-1 to fit the casings programmes of the nearby wells. Table 4 shows the casing design of IDDP-2. The actual result of the casing in IDDP-2 is shown in Figure 5.

Main surprises and achievements of IDDP-2 are as follows (Fridleifsson, 2017):

1) High permeability all the time during drilling; total loss >50 l/s all the time.
2) No drill cuttings were retrieved below 2.5 km (except for 3.0-3.2 km after casing).
3) Without drill cores we would not have known anything about the rock types below 3.2 km and their hydrothermal alteration and metamorphism.

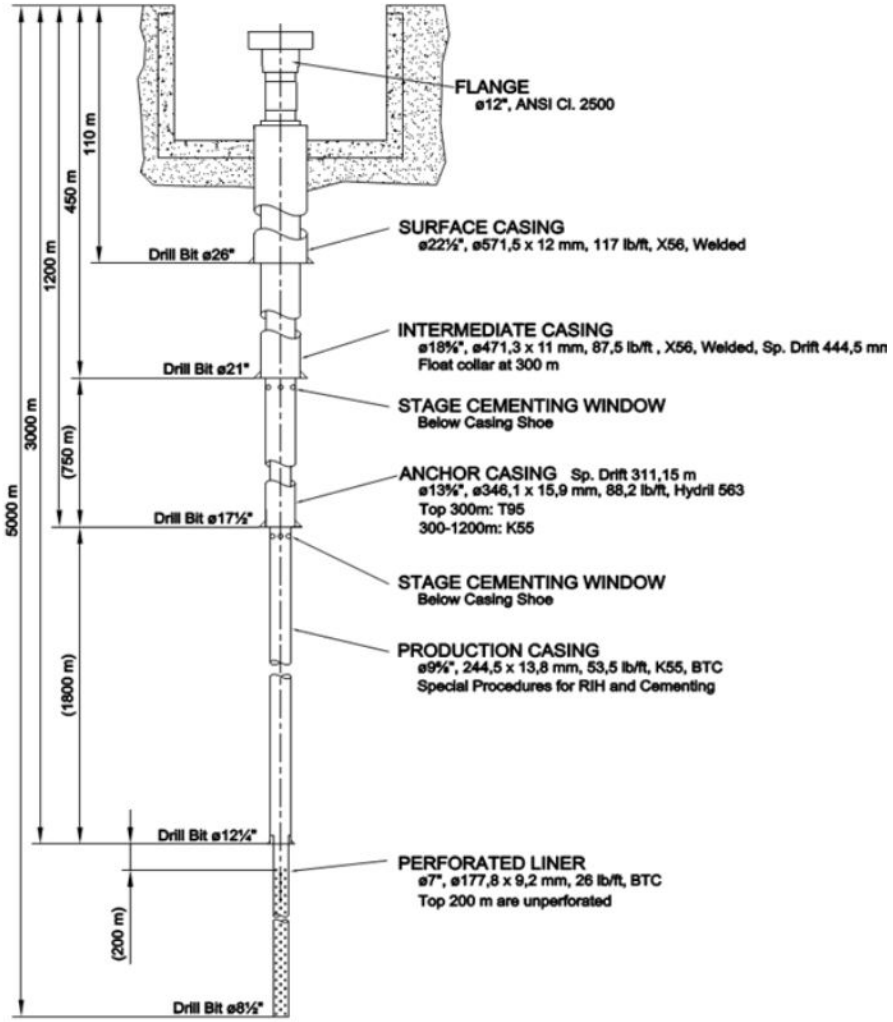

FIGURE 4: Well design of IDDP-2 (Ingason, 2018)

4) The ICDP and NSF funds for coring proved to be of paramount importance for understanding the black smoker analogue rocks at Reykjanes down to the bottom of the well.
5) Geophysical logging below 3.4 km was impossible with conventional equipment because of temperature limitation, LWD tools from Weatherford solved the problem.
6) High permeability at great depths opens new dimensions for re-injection and/or production.
7) Power potential of the deep fluid remains to be studied and evaluated.

TABLE 4: Casing design of IDDP-2 (Fridleifsson, 2017)

Well casings	**Casing design**
RN-15	22 ½"#117.00 lb/ft, 0 - 87 m 18 ⅝"#87.50 lb/ft, 0 - 293 m 13 ⅜"#68.00 lb/ft, 0 - 794 m
IDDP-2	9 7/8"62.80# T95- W/GEOCONN, 0 – 500 m 9 ⅝"47.00# L80 -W/GEOCONN, 500 - 2941 m 7"26.00# L80- W BTC, 2842 - 4606 m 7"#26.00 lb/ft, TN 80HS TSH W/HYDRILL BLUE 0 - 1300 m

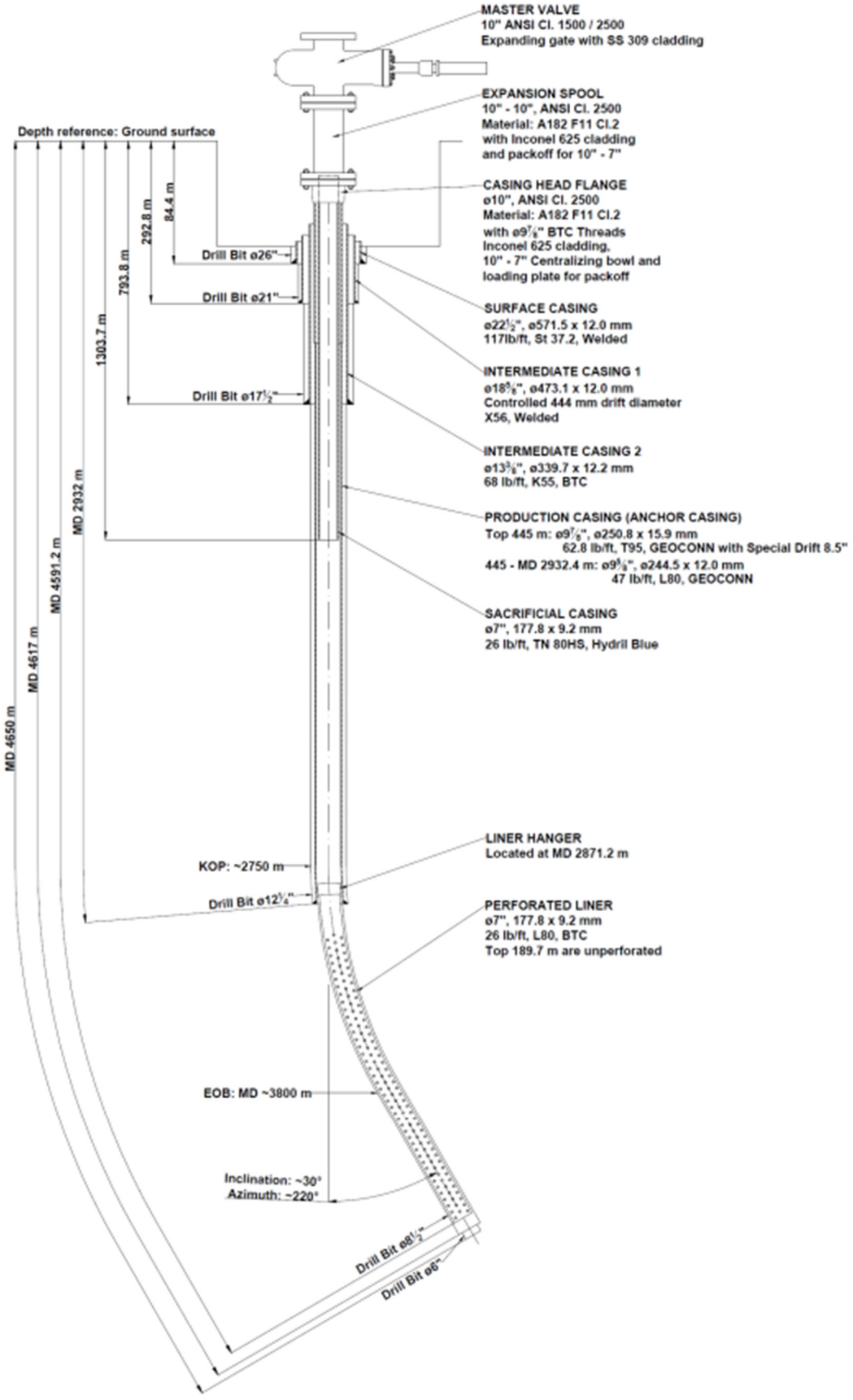

FIGURE 5: Actual well design of IDDP-2 (Weisenberger et al., 2017)

3. BACKGROUND OF STUDY AREA

3.1 Current status of geothermal development

The study area is located in Yangyi Village, Geda Township, Dangxiong County, Tibet Autonomous Region, China, with an average elevation of 4,700 m and 187 km from Lhasa. The Nimu Highway lies east of it, the Zhongni Road in the south, the Qinghai-Tibet Railway in the north, and the famous Yangbajing geothermal field is located 53 km northeast of the area (Figure 6).

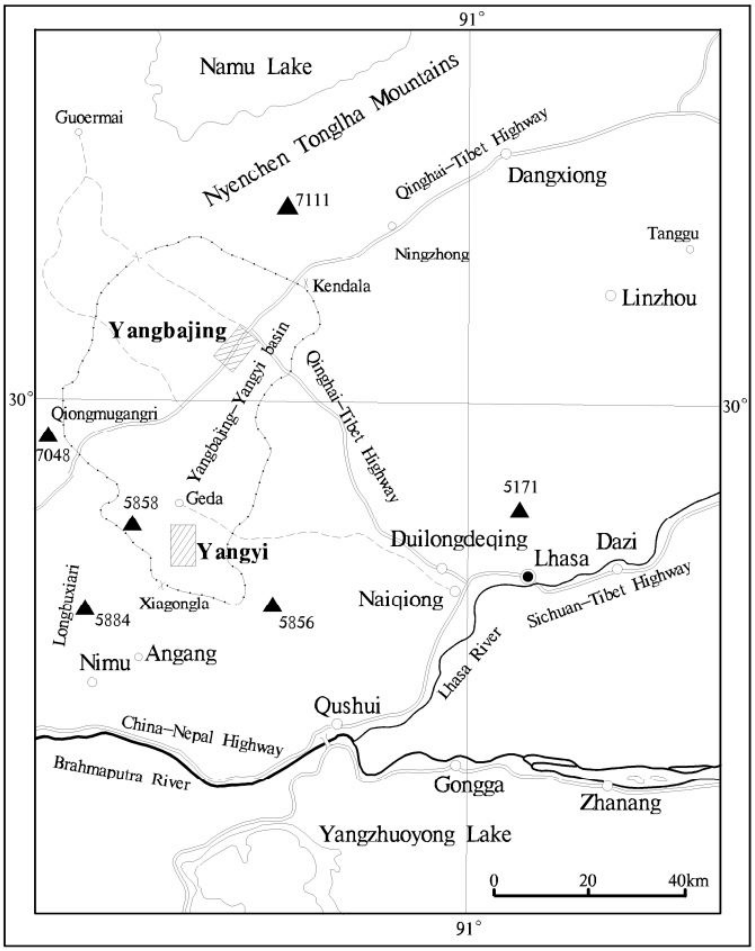

FIGURE 6: Yangyi geothermal field location
(Wang Yanxin and Guo Qinghai, 2010)

In 1985, the Department of Hydrology of the Ministry of Geology and Mineral Resources and the Tibet Geology and Minerals Bureau funded the geochemical exploration and evaluation of the Tibet Yangyi geothermal area. In May that year, the census and detailed investigation were carried out and thermal anomalies were delineated. The scale and prospect of the Yangyi geothermal area were evaluated and exploration drilling started. In 2016, there were 15 geothermal wells in the Yangyi geothermal field with reservoir temperatures of 104-207℃, working temperatures of 105-190℃, closed well pressures of 2.8-9.4 bar and working pressures of 0.95-11.3 bar. The flow rates are 32-373 tons/h and the steam flow rate are 3.5-100 tons/h. The geothermal power potential of the geothermal field is currently 30 MW (IGDCUG, 2014).

3.2 Regional structure

The Yangyi geothermal field is located on the east side of the Gangdise-Nyainqentanglha Mountain Arc Structural Belt . The main structure in the region is fault, followed by fold (Wang Yanxin and Guo Qinghai, 2010). The extension of Tangshan north margin fault in this area and the Xueguqu-Chongbeng fault, respectively, constitutes the east and west boundary faults of the Yangyi and Jidaguo fault basins. They control the formation and development of the fault basins, as well as the distribution and scale of hydrothermal activities.

Tangshan north margin fault constitutes the eastern boundary of the Yangyi and Jidaguo fault basins. It is a normal fault with a westerly dip. The Xueguqu-Chongbeng fault, located in the north at Xueguquto Chongbeng and extending southward to Nimu, and more than 60 km long. It is a N-S trending normal fault with a dip angle of 50°. Width of the fracture zone is about 60 m. A triangular facet of fault had been discovered by Liu Haiyang (2014), on which hormfels and straight fault striations could be seen.

In northern Yangyi there are faults with approximate N-S direction, NW-SE direction and NE-SW direction. These are groups of secondary faults that are generated under the control of boundary faults. They were mainly active during the Miocene period and are all normal, extension faults. The faults have different parameters but the dip angles are all large, generally more than 60° (Liu Haiyang, 2014).

The QiuReGuo anticline consists of tuffaceous glutenite, andesite and sandstone from the Eocene-Oligocene period. The centre (axis) of the anticline is andesitic. The axial strike is 115-120°. The south flank of the anticline has a 155° strike with a dip angle of 54°, and the north flank a 20° strike with a dip angle of 62°. The two flanks are basically mutually geometrically symmetric (Liu Haiyang, 2014).

3.3 Regional stratum

Cenozoic and magmatic rocks are mainly exposed in the area. At the boundary, these are Neogene and Quaternary rocks, widely distributed, while the magmatic rocks consist both of intrusive and extrusive rocks, as well as dykes (Liu Haiyang, 2014).

North of Dalzi, the exposed rocks are mainly Cretaceous. The main stratigraphy of the Upper Cretaceous Naziguo formation (K_2n) is:

1) Variegated conglomerate, glutenite-bearing siliceous rock layer;
2) Gray-green, purple-gray tuffaceous glutenite, sandstone, etc.;
3) Brown red clip gray-green conglomerate, sandstone and mudstone.

The total thickness is 613 m. Intrusive Himalayan period porphyritic granite is found in this formation (Liu Haiyang, 2014).

3.3.1 Magmatic rocks

The regional magmatic rocks consist of intrusive rocks, eruptive rocks, and sporadic distribution of dykes. They are all products of the Himalayan eruption period (Liu Haiyang, 2014):

Magmatic rocks can be found in the mountainous areas on both sides of the Jidaguo and Yangyi basins which were created during the Himalayan period. The main rock types are porphyritic granite and biotite granite.

Extrusive rocks. The effluent rocks in the area are mainly a combination of lava and volcanic clastic rocks. According to the characteristics of volcanic activity and the types of volcanic rocks, the volcanic rocks in the area can be divided into the following lithofacies: overflow facies, eruption facies, and sub-volcanic facies (basic volcanic facies). Among them, the overflow phase is the most common one. According to its lithology, lithofacies and isotopic age, the volcanic rocks in the region can be divided into two sequences, dating from the Eocene-Oligocene period and Miocene-Pliocene period.

Rocks from Eocene-Oligocene period are mainly found in the east of Yangyi and Jidaguo, mainly dacite matrix pyroclastic rocks of explosive facies, and partly volcanic lava. Included are: quartz andesite, andesitic breccia, trachyte, etc. In Lejiemuqu, east Yangyi, the thickness of this volcanic rock layer is about 130 m.

Rocks from the Miocene-Pliocene period are mainly distributed in the west of the Yangyi area. Most of it is lava, which forms an elongated, N-S oriented mountain. These are mainly volcanic lava, sub-volcanic rocks (submerged volcanic rocks) and pyroclastic rocks formed during the continental eruptive phase. Its occurrence is controlled by fracture. In some locations, rocks show varying degrees and different types of alterations due to the effects of hydrothermal activity.

4. DESIGN CONDITIONS FOR PRESSURE AND TEMPERATURE

4.1 Temperature

The temperature assumed as a design condition for the deep well in Yangyi geothermal field is based on temperature loggings of well ZK212. The logging was carried out shortly after the completion of drilling when the formation temperature had not yet recovered. The temperature measurement curve (Figure 7) shows that in the shallow parts (400-500 m and 1000-1200 m) the temperature is obviously lower. This was explained by shallow colder inflow in these depth ranges (Liu Haiyang, 2014). According to the trend seen in the temperature curve in the well, the slope of the deep formation temperature should be steeper. According to general knowledge on high-temperature geothermal resources, the Qinghai-Tibet Plateau, in which the Yangyi area is located, belongs to the intersection of the Indian plate and the Eurasian plate and has the potential to generate high-temperature geothermal resources (Duo Ji, 2003). In the design process, the temperature as a function of depth that is used as a boundary condition is based on the existing logging data while assuming that the function is also linear.

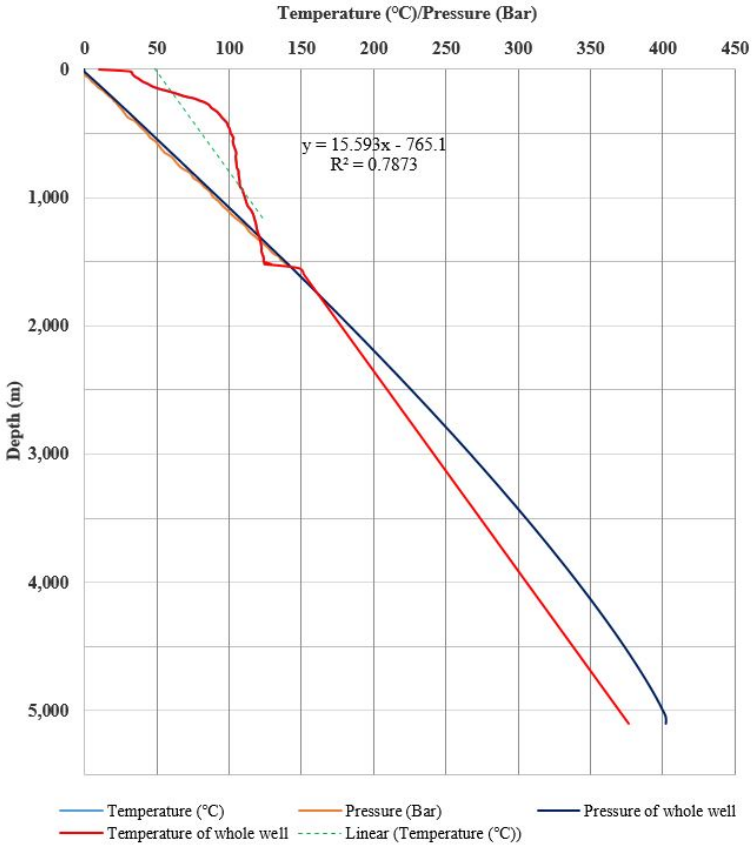

FIGURE 7: T-D and P-D curve of ZK212 and the T-D and P-D simulation curve

The ZK212 well analysed in this study has a depth of 1508 m. Temperature measurements carried out 34 h after the completions of ZK212 showed a temperature of 126°C. By fitting different types of curves, when the R-square value is high with the input X(T) = 374.15 (a minimum for supercritical status), the necessary depth – Y value, is far beyond the reach of general drilling. However, since this study only discusses the method without real values, we use a linear equation with a relatively low R-square value to obtain the equation and the R-square value as shown in Figure 7.

Supercritical conditions are reached when the temperature is greater than 374°C and the pressure above 220 bars, also referred to as the critical point (Huang Hefu, 2000). The formula predicts that the critical temperature is reached in 5028 m depth. Based on the existing data, the well temperature was simulated and pressure calculated to 5,100 m. The result is presented in Figure 7.

4.2 Pressure

The downhole pressure is assumed to be hydrostatic. It is calculated in incremental steps as described in Equation 1. The density, ρ_i is a function of the water temperature. The water level is assumed to be 12 m, the same as elsewhere in the area. The steps in the calculation ($h_i - h_{i-1}$) are 50 m:

$$P_i = P_{i-1} + \rho_{i-1} * g * (h_i - h_{i-1}) \quad (1)$$

Parameters are defined in Nomenclature. The pressure and temperature in well are shown in Figure 7.

4.2.1 Overburden pressure

From older, regional data and the logging data of the formations in the ZK212 well, it is known that there are Tertiary and magmatic rocks from top to bottom. They include coarse shale (with density 2.57-2.80 g/cm^3), tuff (2.50-3.30 g/cm^3), and volcanic breccia and andesite (2.50-3.30 g/cm^3), among others. The thickness is about 280 m. The magmatic rock strata mainly include granite (2.79-3.07 g/cm^3), tuff (2.50-3.30 g/cm^3) and volcanic breccia and quartz rough rock (2.40~2.80 g/cm^3), among others. The density of the rock formation was reviewed and the average rock density is estimated to be 2.50 g/cm^3. The overburden pressure can be calculated according to the following formula:

$$S_v = \rho * g * h \quad (2)$$

where ρ is the rock density at 2.50 g/cm^3, and g is the gravitational acceleration 9.81 m/s^2.

4.2.2 Fracture pressure

When the wellbore is opened, it is filled with drilling fluid which protects and supports the wellbore. However, when the pressure of the drilling fluid column increases to a certain extent, the well wall may crack. The pressure that produces a fractured column is called the formation fracture pressure. In 1969, Eaton published a method for calculating the fracture pressure of the formation. The method evaluates the minimum principal stress when no field data is available from direct measurements. It can be estimated by using the Eaton formula:

$$P_{frac} = P_f + \frac{v}{1-v}(S_v - P_f) \quad (3)$$

where P_{frac} is the minimum principal stress, P_f is the pore pressure (hydrostatic pressure in Section 3.2), S_v is the vertical stress given by the overburden and v is Poisson's ratio (0.35).

4.2.3 Heavy mud pressure

Drilling fluid is circulating working fluid used in the drilling process, commonly known as drilling mud or mud. Mud pressure refers to the pressure per unit area in the wellbore:

$$P_{heavy\ mud} = \rho * g * h \quad (4)$$

where ρ is the density of heavy mud (<1.8 g/cm^3), g is the gravitational acceleration (9.81 m/s^2) and h is the height of the mud column.

4.2.4 Cold water pressure

In the process of geothermal well drilling, the drilling fluid is changed from mud to water when entering the target layer. Now the pressure born by the stratum comes from water in the wellbore:

$$P_{cold\ water} = \rho * g * h \quad (5)$$

where ρ is the density of water (1000 kg/m^3), g is the gravitational acceleration (9.81 m/s^2), and h is the height of the water column.

4.2.5 Saturation vapour pressure

Saturation vapour pressure is the pressure of vapour which is in equilibrium with its liquid (e.g. steam with water). Specifically, it is the maximum pressure possible in water vapour at a given temperature.

The saturated vapour pressure under different temperature conditions is listed in the handbook for properties of water.

5. WELL DESIGN

5.1 Setting casing depths

For the design of a deep well in Yangyi geothermal field, the New Zealand Geothermal Well Design Standard (NZS 2403:2015) is used, and combined with the successful design experience of geothermal wells in the Iceland IDDP project. using the formulae above, each relevant pressure is calculated using known parameters as boundary conditions, and the associated curves drawn (Figure 8).

The temperature and pressure conditions at 5100 m depth are that the fluid phase is liquid and the bottom hole pressure is 40.22 MPa. When the fluid rises to 2400 m, the fluid pressure is gradually reduced to 21.57 MPa, the fluid begins to boil and eventually reaches the surface. In Figure 8, we can see that the pressure curve intersects the cold-water curve at roughly 2200 m depth which is therefore the minimum depth of the production casing, assuming only water will be used as drilling fluid when drilling the production part of the well.

The goal of drilling a well similar to the IDDP wells is to produce superhot fluid. Here, we assume the fluid temperature to be over 300°C. The temperature profile in Figure 7 indicates that 300 °C is reached at about 3900 m depth. To case out colder aquifers the production casing must therefore be 3900 m deep.

The temperature and pressure at 3900 m depth imply that the fluid is liquid, and the bottom hole pressure is 33.44 MPa. When the fluid rises to 890 m, the fluid pressure is gradually reduced to 8.16 MPa and

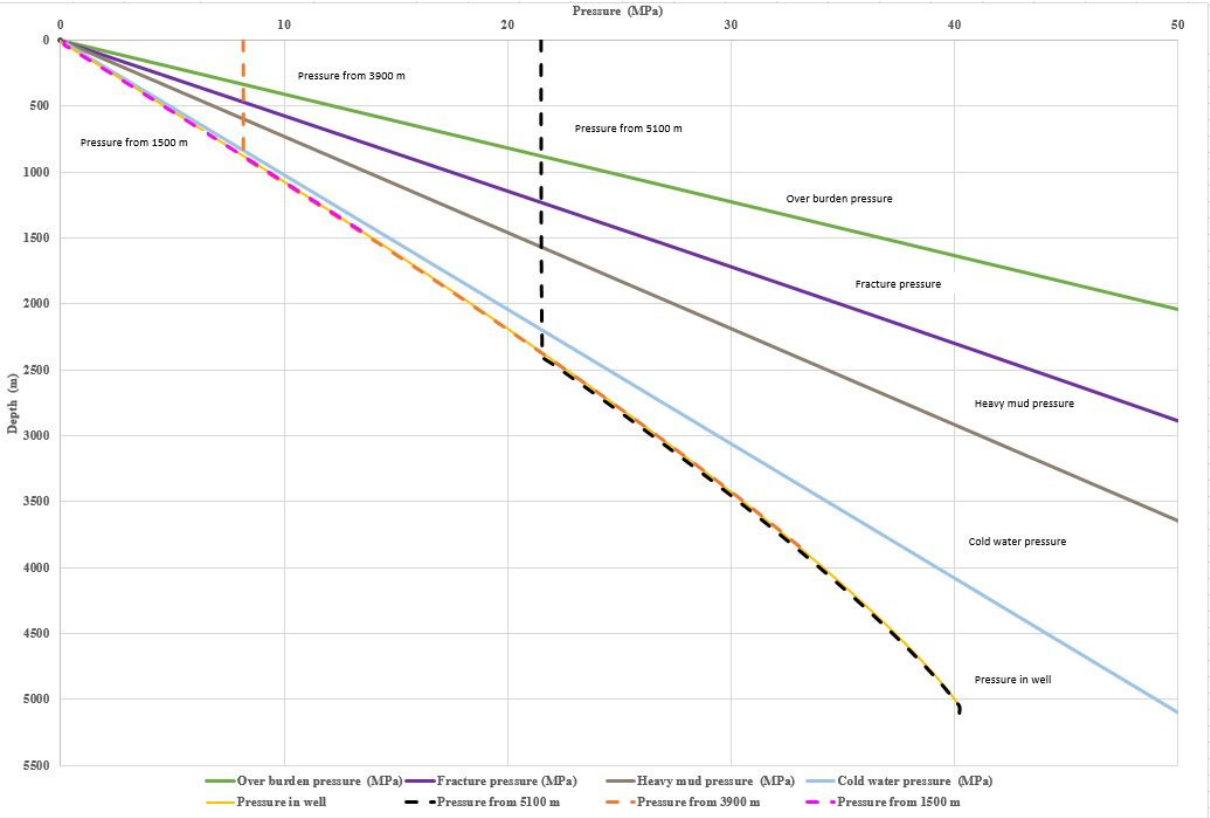

FIGURE 8: Different hypothetical pressure curves for the hypothetical DDP well

the fluid begins to boil and eventually reaches the surface. In Figure 8, one can see that the pressure curve intersects the heavy mud curve at roughly 600 m depth, which is therefore the minimum depth of anchor casing, assuming mud will be used as drilling fluid when drilling. From an engineering point of view, it is however unrealistic to drill an open hole from 600 m down to 3900 m. The depth of the anchor casing is therefore decided to be 1500 m.

Based on experience from drilling other wells in the area, we know that by drilling and cementing a 180 m surface casing, a 1500 m well can be drilled.

5.2 Casing diameter

The casing and the wellbore sizes are generally decided on layer by layer from the inside to the outside. First, the size of the production casing needs to be determined, and then the casing size of each layer and the corresponding wellbore size are determined. The sizes of the wellbore at the surface and of the conduit are calculated last. Figure 9 shows the selection of the casing and wellbore (bit) dimensions in the industry standard. When using this roadmap, the final casing size is determined first. The solid arrows represent the usual fit which has enough clearance to fit into the casing and inject cement. Dotted arrows indicate unconventional fits. When using the combination shown by the dashed line, the effects of casing coupling, drilling fluid density, cementing measures, and wellbore curvature on the quality of the casing and cementing must be fully noted.

A production part having a diameter of 8½ ” is adequate for the type of well that is being discussed here. The other diameters of the well are decided based on that. Combining the results of casing depth and the results of the casing and wellbore (bit) size matching roadmap, we obtain the results of the casing depths and casing sizes shown in Table 5.

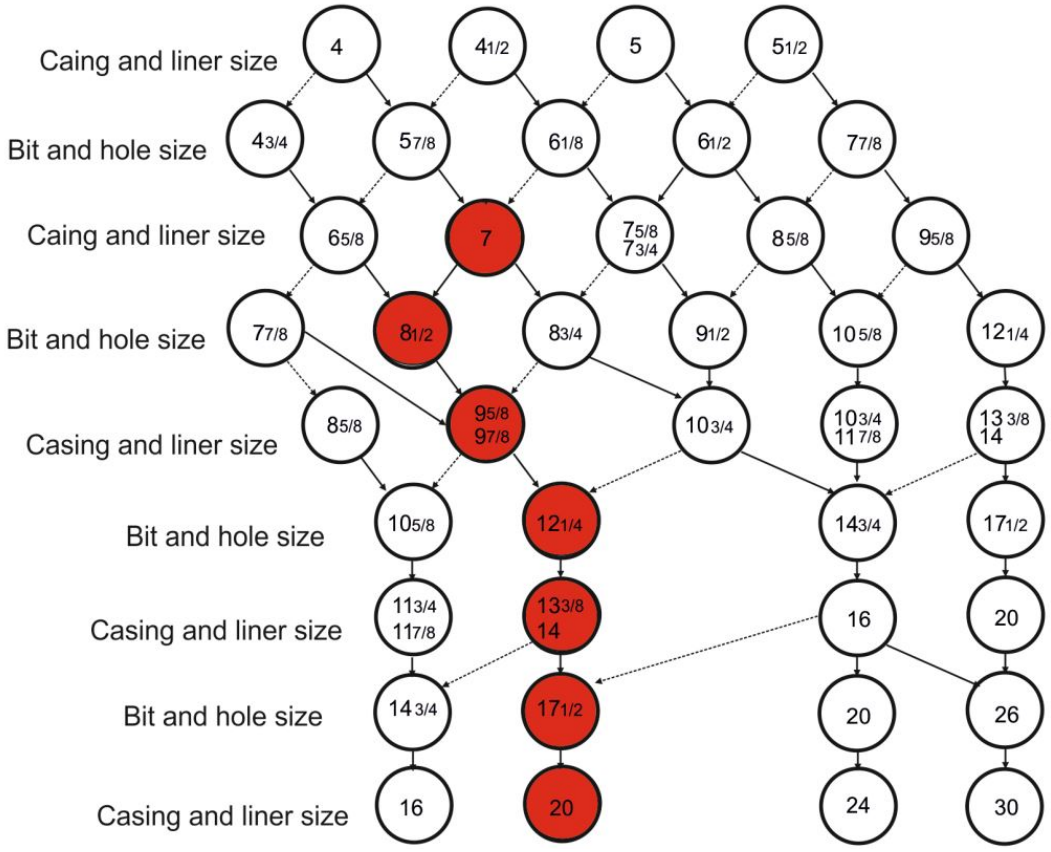

FIGURE 9: Casing and wellbore (bit) size matching roadmap

TABLE 5: Casing depth and casing size for the DDP well

Casing name	Casing depth (m)	Casing size (")
Conductor casing	20	26
Surface casing	180	20
Anchor casing	1500	13 ⅜
Production casing	3900	9 ⅝
Slotted liner	5100	7

5.3 Design calculations

After determining the minimum depth of each casing through various fluid and steam pressures in the formation and the wellbore, the weight, grade and other parameters of the casing are calculated according to the relevant calculation formula of the NZS 2403:2015 standard (NZS, 2015). The most suitable casings are selected based on the calculation results. Appendix I shows tables with results of calculations on strength of casings for various cases.

The casing diameter has been selected as shown with red/dark colour in Figure 9. The casing dimensions for each class are: 22" conductor casing, 20" surface casing, 13⅜" anchor casing, 9 ⅝" production casing, and 7" slotted liner. Tentatively, the steel grade of K55 is chosen. If the calculation result does not meet the design requirements, the strength of the steel grade is increased until it meets them.

5.3.1 Axial loading before and during cementing

Until the annular cement sets around the casing, the tensile force at any depth is calculated by considering the weight of the casing materials in air plus the weight of the casing contents less the buoyant effect of any fluid displaced by the casing (Equations 6-9). The calculation results are shown in Table 6.

$$F_{\text{hookload}} = F_{\text{csg air wt}} + F_{\text{csg contents}} - F_{\text{displaced fluids}} \tag{6}$$

$$F_{\text{csg air wt}} = L_z \cdot W_p \cdot g \times 10^{-3} \tag{7}$$

$$F_{\text{csg contents}} = \sum \rho_{if} \cdot L_{if} \cdot \frac{\pi d^2}{4} \cdot g \times 10^{-6} \tag{8}$$

$$F_{\text{displaced fluids}} = \sum \rho_{ef} \cdot L_{ef} \cdot \frac{\pi D^2}{4} \cdot g \times 10^{-6} \tag{9}$$

The calculation formula of axial loading before and during cementing is as shown above in Equations 6-9, and the calculation results are shown in Table 6.

TABLE 6: Calculation result of axial loading before and during cementing

Grade	K55	K55	T95
Casing size (")	20	13 ⅜	9 ⅝
F_{hooklood} (MN)	0.6	2.4	3.9

5.3.2 Tensile force during running and cementing casing

The formula of tensile force during running and cementing casing is as shown below (Equation 10) and the results of the calculations are shown in Table 7:

$$\text{Design factor} = \frac{\text{minimum tensile strength}}{\text{maximum tensile load}} \geq 1.8 \quad (10)$$

TABLE 7: Calculation results of tensile force during running and cementing casing

Grade	K55	K55	T95
Casing size (")	20	13 ⅜	9 ⅝
Calculation factor	1.5	2.3	1.9

5.3.3 Tension at the top of any string anchoring a wellhead against lifting force by fluid in the well

The formulae to calculate tension at the top of any string anchoring a wellhead against the lifting force of fluid in the well are shown below (Equations 11-12). The results of calculation are shown in Table 8:

$$F_w = \frac{\pi}{4} \times P_w \times d^2 \times 10^{-3} - F_m \quad (11)$$

$$\text{Design factor} = \frac{\text{minimum tensile strength}}{\text{maximum tensile load}} \geq 1.8 \quad (12)$$

TABLE 8: Calculation result of tension at the top of any string anchoring a wellhead against lifting force of fluid in the well

Grade	C90
Casing size (")	13 ⅜
Calculation factor	3.6

5.3.4 Thermal load on anchor casing (where applicable)

Formula for the thermal load on anchor casing (where applicable) is as shown below (Equation 13), the calculation results are shown in Table 9.

$$\text{Design factor} = \frac{\text{anchor casing tensile strength}}{\text{rising casing compressive load}} \geq 1.4 \quad (13)$$

TABLE 9: Calculation result of thermal load on anchor casing

Grade	C90
Casing size (")	13 ⅜
Calculation factor	8.5

5.3.5 Extreme fibre compressive stress in an uncemented liner due to axial self-weight and helical buckling

Extreme fibre compressive stress in an uncemented liner due to axial self-weight and helical buckling formulae are shown below (Equations 14-15), and the calculation results are shown in Table 10.

$$f_c = L_z \times W_p \times g \times \left[\frac{1}{A_p} + \frac{De}{2l_p}\right] \quad (14)$$

$$\text{Design factor} = \frac{\text{minimum yield stress} \times R_j}{\text{total compressive stress}} \geq 1.0 \quad (15)$$

R_j should be equal or less than 1.0

TABLE 10: Calculation result of extreme fibre compressive stress in an uncemented liner due to axial self-weight and helical buckling

Grade	K55
Casing size (")	7
Calculation factor	2.7

5.3.6 Maximum differential burst pressure of string during cementing near shoe or stage cementing ports

The formulae for the maximum differential burst pressure of string during cementing near shoe or stage cementing ports are shown below (Equations 16-17), and the results of the calculation in Table 11.

$$\Delta P_{internal} = [L_z \rho_c - L_f \rho_f] \times g \times 10^{-3} \quad (16)$$

$$\text{Design factor} = \frac{\text{internal yield pressure}}{\text{differential internal pressure}} \geq 1.5 \quad (17)$$

TABLE 11: Calculation result of maximum differential burst pressure of string during cementing near shoe or stage cementing ports

Grade	K55	C90	T95
Casing size (")	20	13 ⅜	9 ⅝
Calculation factor	12.7	2.3	2.8

5.3.7 Maximum differential burst pressure at the surface (after cementing)

Two cases need to be considered:

I. With steam at the wellhead, the coefficients of design are as given in Equation 18, and the calculation results in Table 12:

$$\text{Design factor} = \frac{\text{internal yield pressure} \times R_i}{\text{differential internal pressure}} \geq 1.8 \quad (18)$$

TABLE 12: Calculation result of maximum differential burst pressure at the surface (after cementing)

Grade	C90	T95
Casing size (")	13 ⅜	9 ⅝
Calculation factor	1.8	2.8

II. With cold gas at the wellhead, the stress corrosion tensile limit of the steel should be used to determine the appropriate yield strength.

5.3.8 Biaxial stress if wellhead is fixed on the casing (combined effects of axial and circumferential tension)

The formulae for the biaxial stress if the wellhead is fixed on the casing (combined effects of axial and rent tension) and the coefficient of the design are as shown below (Equations 19-20). The results are shown in Table 13.

$$f_t = \frac{\sqrt{5}}{2} \times \left(\frac{P_w \times d}{D - d}\right) \tag{19}$$

$$\text{Design factor} = \frac{\text{steel yield pressure}}{\text{maximum tensile pressure}} \geq 1.5 \tag{20}$$

TABLE 13: Calculation result of biaxial stress if wellhead is fixed on the casing

Grade	C90
Nominal size (")	13 ⅜
Calculation factor	2.2

5.3.9 Hoop stressing (collapse) during casing cementing operations

The formulae for hoop stressing (collapse) during casing cementing operations and design coefficients are shown below (Equations 21-22). The results are shown in Table 14.

$$\Delta P_{external} = (L_z \rho_c - L_z \rho_f) \times g \times 10^{-3} \tag{21}$$

$$\text{Design factor} = \frac{\text{pipe collapse pressure}}{\text{differential external pressure}} \geq 1.2 \tag{22}$$

TABLE 14: Calculation result of hoop stressing (collapse) during casing cementing operations

Grade	K55	C90	T95
casing size (in)	20	13 ⅜	9 ⅝
Calculate factor	6.6	2.2	2.5

5.3.10 Hoop stressing (collapse) – during production operations, annulus is at formation pressure

The formulae for hoop stressing (collapse) during production operations while the annulus is at formation pressure and design coefficients are shown below (Equations 23-24). The results are as shown in Table 15.

$$P_z = P_f \tag{23}$$

$$\text{Design factor} = \frac{\text{pipe collapse pressure}}{\text{differential external pressure}} \geq 1.2 \tag{24}$$

TABLE 15: Calculation result of hoop stressing (collapse) –during production operations, annulus is at formation pressure

Grade	C90	T95
casing size (in)	13 ⅜	9 ⅝
Calculated design factor	1.8	2.0

5.4 Casing materials and properties

5.4.1 Casing grade

Steel casings should be selected from API Spec 5CT or API Spec 5L. While low alloy steel is the predominant material used for casing, special conditions (particularly severely corrosive exposure) could warrant consideration of other products (Ingason, 2018).

In situations where gas may be present, casing materials have to be selected in order to minimise the possibility of failure by hydrogen embrittlement or sulphide stress corrosion. For increased resistance to H_2S attack, materials should be selected that are approved or conform to ANSI/NACE MR 0175/ISO 15156. Such approved API steels are:

Spec 5CT grades: H-40, J-55, K-55; M65, L-80 type 1, C90 type 1, T95 type 1

Spec 5CT grades: A and B and X-42 through X-65

5.4.2 Connections

Ingason (2018) summarizes the usage of connections in the following way:

1) Buttress threads are most commonly used;
2) VAM threads are sometimes used;
3) API round threads are seldom used;
4) Special "proprietary" or "premium" connections (e.g. Hydril – now Tenaris) are sometimes used for improved strength/sealing or to reduce clearance between casing OD and well ID, e.g. for slotted liners;
5) GeoConn is a Buttress type thread which has superior strength as there is no gap between the casing ends;
6) Surface casings of a large diameter are sometimes butt welded. In Iceland also the anchor casing down to ~350 m depth is in some cases welded. Requires certified welders and testing; and
7) Welding (slip on welding-SOW) is often used for casing heads. Requires heating and post weld treatment. Note: Most high-grade casing steels (>K55) are difficult to weld.

5.4.3 Effect of temperature on casing properties

Unless other values apply to specific steels, the coefficient of thermal expansion for casings (α) is (NZS, 2015):

13×10^{-6}/°C.

The Young's modulus for casing steel is: $E = 210 \times 10^3$ MPa. If no other data is available, a conservative estimate for stress caused by thermal expansion is:

$210\times10^3 \times 13\times10^{-6} = 2.73$ MPa/°C

The casing string material tensile yield and ultimate strengths are de-rated at elevated temperatures, as listed in Table 16.

TABLE 16: Effect of temperature on casing properties (NZS 2403:2015)

Grade	Temperature (°C)						
	20	**100**	**150**	**200**	**250**	**300**	**350**
API yield strength (factor)							
J55/K55	1.00	0.94	0.90	0.90	0.85	0.80	0.70
L80/C90/T95	1.00	0.96	0.92	0.90	0.88	0.85	0.81
Tensile strength (factor)							
All grade	1.00	0.96	0.92	0.90	0.88	0.86	0.84
Modulus of elasticity (103 MPa)							
All grade	210	205	201	197	194	190	185

Eventually, this results in the well design for a DDP well in Yangyi geothermal area (Figure 10).

6. CEMENTING

Three casing cementing operations are usually performed while drilling a geothermal well. They are for cementing:

a) Surface casing;
b) Anchor casing; and
c) Production casing.

Occasionally, the production liner or tieback casing is also cemented (Guerra Guerrero, 1998).

Cementing is a process in which cement slurry is injected into the annulus between the well wall and the casing to consolidate the casing string and the formation rock (Guan Zhichuan and Chen Tinggen, 2016). Three main methods are used to pump the cement into the space between the formation and the casing (Hole, 2008a).

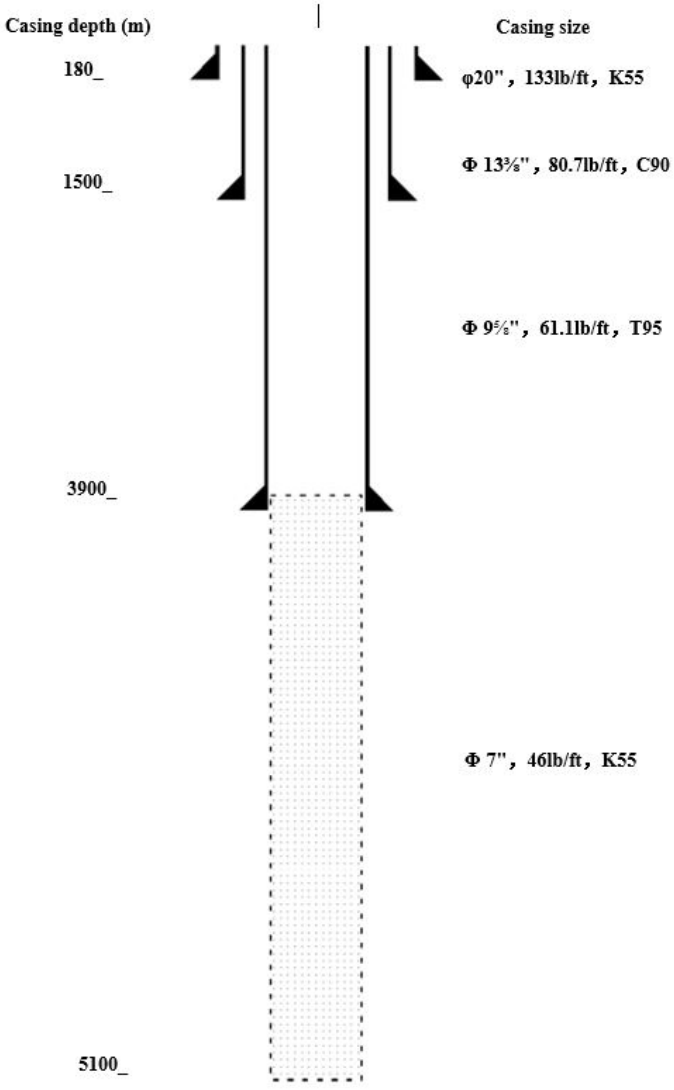

FIGURE 10: Well design for a DDP well in Yangyi geothermal area

6.1 Conventional cementing

The first and most common technique of cementing is to pump cement into the casing through a cement head attached to the top of the casing. A certain volume of cement slurry is pumped and the cement slurry is displaced from the casing into the annulus. Plugs are used to separate the cement slurry from the fluid in the casing and the displacement fluid.

6.2 Inner string cementing

The second technique，the ‘Inner String’ cementing technique, requires a cementing string to be run inside the casing and ‘stabbed’ into a receptacle in the float collar, which is usually located at the top of the first or second casing joint. The cement slurry is then pumped through the cementing string, through the ‘shoe track’ (the one or two joints of casing at the bottom of the casing string), and directly to the annulus. The small volume of the cementing string allows cement slurry to be mixed and pumped until cement slurry is returned to the surface from the annulus. The volume to be mixed and pumped does not have to be finite.

An inner string method is commonly used to cement large size casings run below 1000 m and has many advantages. Large cement heads and plugs are not required during the construction preparation phase. This method can reduce the time and pressure of cement displacement during construction. Most important is the reduction of pollution of the reservoir by the cement and to allow the cement to return faster from the outside of the casing.

6.3 Reverse circulation cementing

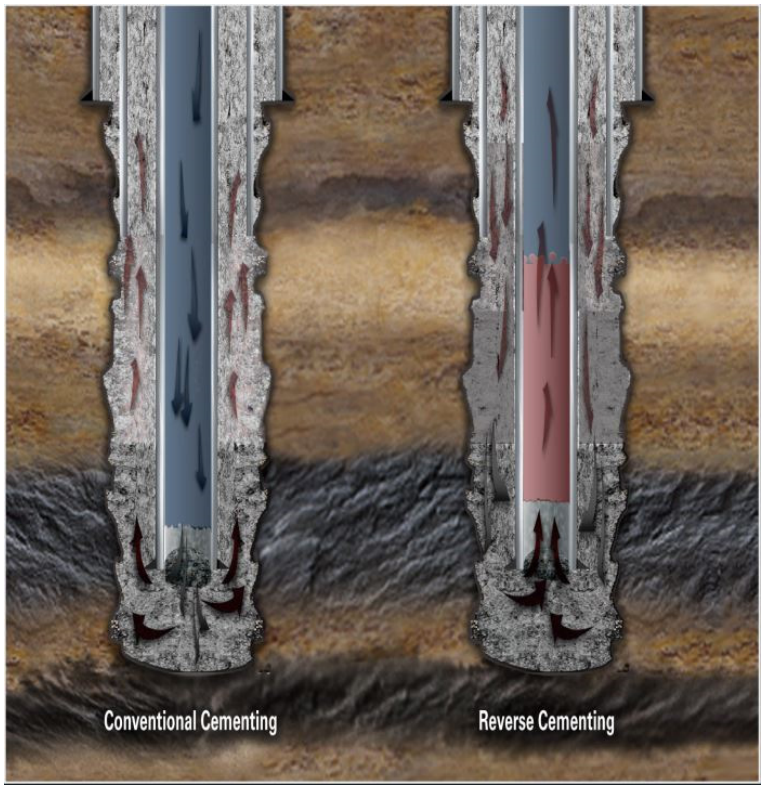

FIGURE 11: Conventional vs. reverse cementing (Hernández et al., 2010)

The third technique, 'reverse circulation', involves pumping the cement slurry directly to the annulus, with the displaced fluid being forced back through the casing shoe and through the casing to the surface (Figure 11). This technique is rarely utilised because in the case of circulation loss there is no possibility to ensure if the casing shoe has been cemented.

6.4 Multiple-stage cementing

Multiple-stage cementing tools are recommended for the following circumstances (Halliburton, 2018):

1) Wells where the hydrostatic head of the cement is greater than the formation pressure in some intervals but not in other intervals.
2) Lighter-weight cement would be required in low-pressure formation sections in order to avoid breakdown of the formation and reduce the potential for lost circulation.
3) Heavier-weight cement would be required in high-pressure formation sections in order to maintain control of the well.
4) In deep, hot holes where time to pump the desired quality and quantity of cement is limited and thus slurry pump ability is best maintained by reducing the total volume to be placed in an interval during any particular pumping operation.
5) When only certain portions of the wellbore require zonal isolation.
6) In downhole conditions that require different slurry blends to address unique challenges to each segment and achieve the intended zonal-isolation integrity.
7) In horizontal wells where the bend radius of the well requires cementing.

Because of the big depth and limited pump ability, it is possible to use two-stage cementing in Yangyi geothermal area (Figure 12).

This cementing procedure is used when the pumping rate is low, pump pressures are high or the hydrostatic pressure exceeds the fracture pressure of some of the formations. The operation is split into two stages (Bett, 2010):

1) *First stage*: this part is similar to single-stage cementing except that a bottom plug is not used. Instead, a special plug is used to pass freely through the stage collar. The first stage is performed after the cement plug lands on the landing collar.
2) *Second stage*: this final part requires the use of a stage collar which allows pumping cement from the inner part of the casing string into the annulus. The openings in the stage collar are sealed off by the inner sleeve. When the first stage is completed, a special dart is dropped from the surface

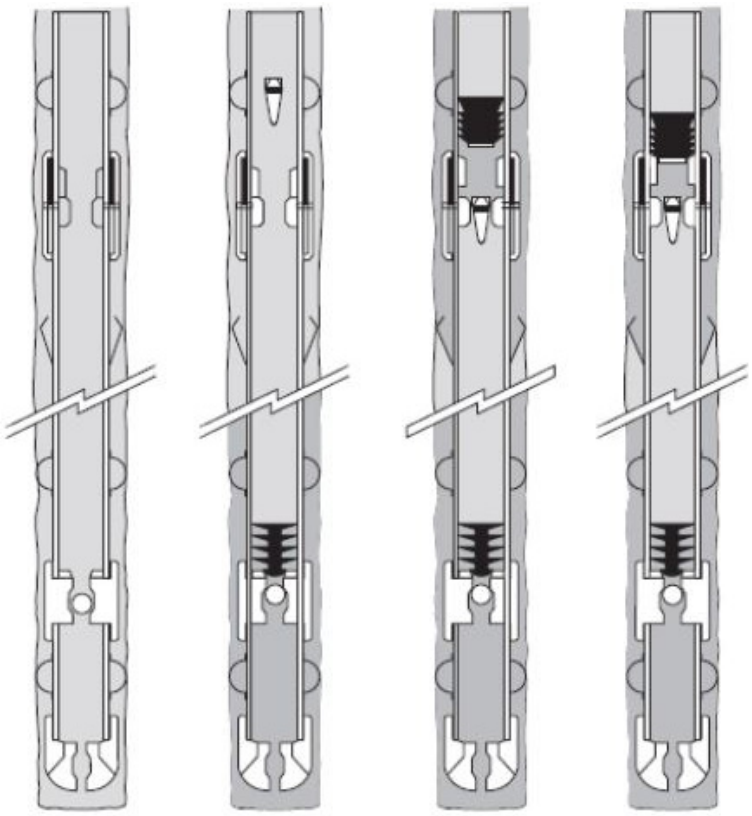

FIGURE 12: Four steps of multi-stage cementing. The first stage is performed after the cement plug lands at the landing collar. In the second stage, a special dart is dropped from the surface and lands in the inner sleeve. The annulus is cemented, then a cement plug is dropped and displaced by drilling fluids (Nelson, 1990, Khaemba, 2016)

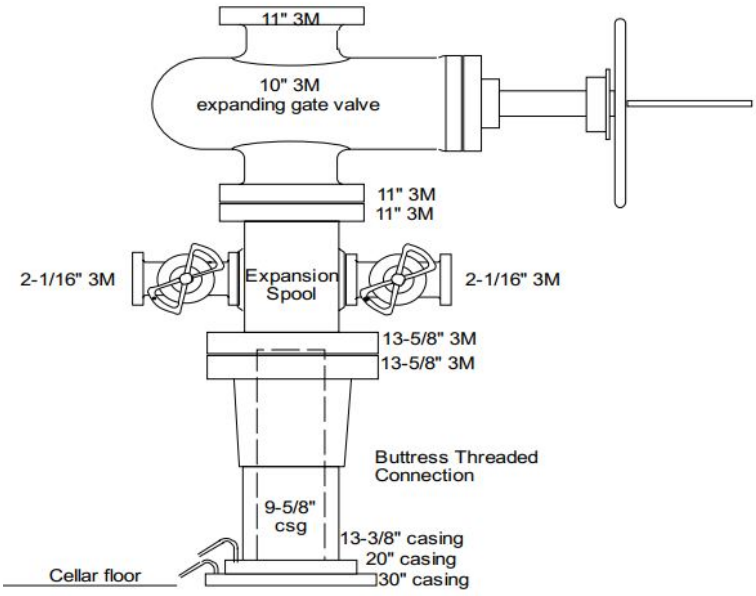

FIGURE 13: Typical completion wellhead (Hole, 2008b)

and lands in the inner sleeve. Then, the pressure is increased above the dart to open the ports. The annulus is cemented by pumping slurry through the ports, then a cement plug is dropped and displaces drilling fluids till it lands on the stage collar, then the casing string is pressure tested.

7. WELLHEAD

After Hagen Hole (2008b) studied the wellhead, he summarized that the characteristics of the permanent wellhead components are as following:

1. Casing head flange (CHF):
Usually, and preferably, attached to the top of the anchor casing, but in some instances directly attached to the top of the production casing. The casing head flange may incorporate side outlets to which side valves are attached.

2. Double flanged expansion/ adaptor spool:
Side outlets may be incorporated in the expansion spool (as an alternative to those on the CHF).

3. Master valve
A typical wellhead assembly for a 'standard' well completed with an 8 ½" diameter production hole section, 9 ⅝" production casing and 13 ⅜" anchor casing is illustrated schematically in Figure 13.

The expected pressure and temperature at the wellhead under this condition is 21.5 MPa and 372°C (Figure 14). The most suitable wellhead is a Class 2500 master valve.

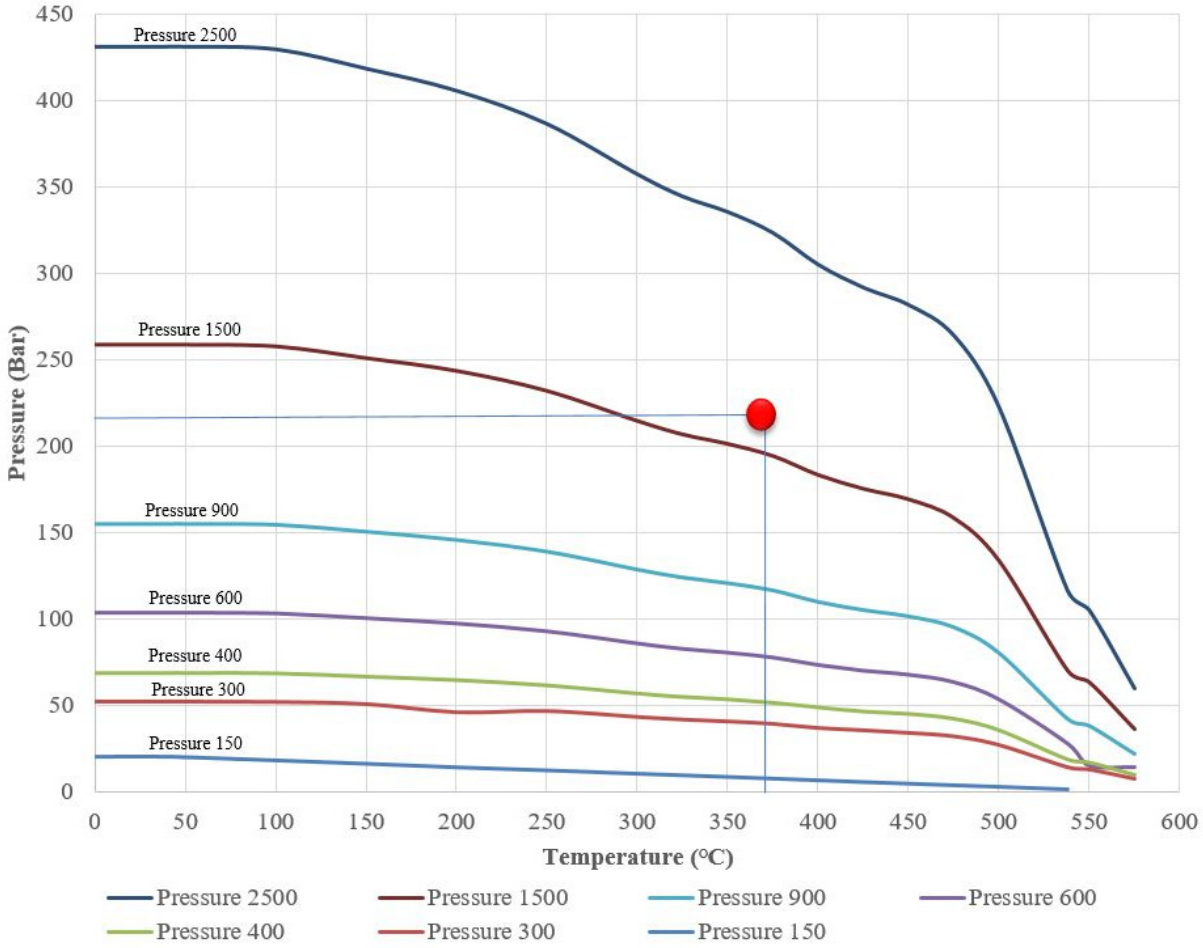

FIGURE 14: Working pressure by classes

8. CONCLUSIONS

1) In the design of IDDP project, the designer utilizes the relationship between cold water pressure and depth, mud pressure and depth, as well as between saturated steam pressure and depth at different casing depths to develop the minimum casing depth design.

2) Conditional fitting of the ZK212 well indicates that when the depth reaches 5100 m, the bottom hole temperature is 376 °C and the bottom hole pressure approx. 40 MPa.

3) Applying the design method described above to the geology of the Yangyi area yields the following results: target depth 5100 m, conductor casing depth 20 m, surface casing depth 180 m, anchor sleeve depth 1500 m and production casing depth 3900 m.

ACKNOWLEDGEMENTS

First of all, I would like to sincerely thank Mr. Lúdvík S. Georgsson, Director of UNU-GTP, and Mr. Ingimar G. Haraldsson, Deputy Director of the UNG-GTP, for giving me the opportunity to participate in the 6-month geothermal training event. I would like to extend my gratitude to the other UNU-GTP staff members: Ms. Thórhildur Ísberg - School Manager, thank you for guiding me step by step through training related matters, Ms. Málfrídur Ómarsdóttir - Environmental scientist, thank you for taking care of us when we are in field trips. Thank you for your help in the report format modification. And Mr. Markús A. G. Wilde - Service Manager, thank you for providing us with all kind of helpful information. Thanks to ISOR instructors and lecturers for their hard work, guidance and sharing of valuable knowledge.

I would like to sincerely thank Mr. Kristinn Ingason, who met me regularly during busy work and told me about the technical details that the project design needed to consider, providing meticulous explanations and patient guidance for my project report writing. His profound knowledge and easy access to people deserve my admiration. I would also like to thank Mr. Thóroddur Sigurdsson for his advice on my project report.

I would like to thank all the UNU Fellows of 2018. In the process of getting along, we learn from each other, understand each other, help each other, widen our horizons, increase our mutual friendship. I hope that our friendship lasts forever. At the same time, I would also like to thank Ms. Zheng Tingting for her help and encouragement during my study in Iceland.

I would like to thank my employer, Sinopec Green Energy Geothermal Development Co., Ltd for providing financial support for my training. And thank the company's leaders for their concern, support and visits.

Finally, I would like to thank my family, especially my wife, Ms. Li Jiao, for her support and understanding during the period when I could not accompany her. And my baby son, you have always been the source of my motivation.

NOMENCLATURE

$\mathbf{P}_{frac}$	=	In situ fracture pressure of a formation (MPa);
$\mathbf{P}_f$	=	Pore pressure (MPa) – assumed to be the boiling point pressure;
V	=	Poisson's ratio values, averaged from the values of Gercek (2007);
Sv	=	Overburden pressure (vertical pressure due to the weight of overlying formations (MPa));
ρ (z)	=	Density of the overlying rock (kg/m^3);
z	=	Depth (m);
$\mathbf{F}_{csg\ air\ wt}$	=	Air weight of casing (kN);
$\mathbf{F}_{csg\ contents}$	=	Weight of internal contents of casing (kN);
$\mathbf{F}_{displaced\ fluids}$	=	Weight of fluids displaced by casing (kN);
$\mathbf{F}_{hookload}$	=	Surface force suspending casing that is subjected to gravitational and static hydraulic loads (kN);
$\boldsymbol{\rho}_{if}$	=	Density of a section of fluids with constant density within a casing (kg/l);
$\boldsymbol{\rho}_{ef}$	=	Density of a section of fluids with constant density within an annulus (kg/l);
$\mathbf{L}_{if}$	=	Vertical length of a section of fluid having the same density – within the casing (m);
$\mathbf{L}_{ef}$	=	Vertical length of a section of fluid having the same density – within the external annulus (m);
$\mathbf{L}_z$	=	Depth of casing (m);
$\mathbf{L}_f$	=	Height above casing shoe of cement column inside casing (m);

$\mathbf{W_p}$ = Unit weight of casing (kg/m);
$\mathbf{D}$ = Casing outside diameter (mm);
$\mathbf{d}$ = Casing inside diameter (mm);
$\mathbf{g}$ = Acceleration due to gravity (9.81 m/s^2);
$\mathbf{F_p}$ = The tensile force at the surface from casing weight (kN);
$\mathbf{L_w}$ = Depth of water level in well (m);
$\mathbf{A_p}$ = Cross-sectional area of pipe (mm^2);
$\mathbf{n}$ = Mean specific volume of hot fluid (m^3/kg);
$\mathbf{f_b}$ = Maximum stress due to bending (MPa);
$\mathbf{E}$ = Modulus of elasticity (MPa);
$\mathbf{q}$ = Curvature of deviated hole (° per 30 m);
$\mathbf{F_c}$ = Compressive force due to heating (kN);
$\mathbf{F_r}$ = Resultant axial force (kN);
$\mathbf{T_1}$ = Neutral temperature (temperature of casing at the time of cement setting) (°C);
$\mathbf{T_2}$ = Maximum expected temperature (°C);
$\mathbf{a}$ = Coefficient of linear thermal expansion (°C^{-1});
$\mathbf{F_t}$ = Tensile force due to cooling (kN);
$\mathbf{T_3}$ = Minimum temperature after cooling well (°C);
$\mathbf{F_w}$ = Lifting force due to wellhead pressure (kN);
$\mathbf{P_w}$ = Maximum wellhead pressure (MPa);
$\mathbf{F_m}$ = Net downward force applied by the wellhead due to its own mass and pipe work reactions (kN);
$\mathbf{f_c}$ = Total extreme fibre compressive stress due to axial and bending forces (MPa);
$\mathbf{e}$ = Eccentricity (actual hole diameter minus D) (mm);
$\mathbf{I_p}$ = Net moment of inertia of the pipe section, allowing for slotting or perforating (mm^4);
$\mathbf{R_j}$ = The connection joint efficiency;
$\mathbf{\Delta P_{internal}}$ = Differential on casing during cementing (MPa);
$\mathbf{L_f}$ = Total vertical length of fluid column in an annulus (m);
$\mathbf{\rho_c}$ = Cement slurry density (1.87 kg/l);
$\mathbf{\rho_f}$ = Density of water in annulus (kg/l);
$\mathbf{R_i}$ = Temperature reduction factor (ratio);
$\mathbf{F_t}$ = Maximum tensile stress (MPa);
$\mathbf{P_w}$ = Maximum wellhead pressure (MPa);
$\mathbf{\Delta P_{external}}$ = Differential pressure on casing during cementing (MPa).

REFERENCES

Bett, E.K., 2010: Geothermal well cementing, materials and placement techniques, Report 10 in: *Geothermal Training in Iceland*, UNU-GTP, Iceland, 99-130.

Duo Ji., 2003: Typical high temperature geothermal system - the basic characteristics of Yangbajing geothermal field. *Engineering Science, Beijing, 5-1*, 42-43.

Eaton, B.A., 1969: Fracture gradient prediction and its application in oilfield operations. *J.P. Technology, 21-10*, 25-32.

Fridleifsson, G.Ó., 2017: Recent updates from the world's hottest geothermal energy drilling. *Proceedings of the CGER conference*, webpage: cger.no/doc//pdf/presentations%20GeoEnergi2017/01-Gudmundur-GeoEnergy-key%20note-to%20web.pdf

Fridleifsson, G.Ó., and Albertsson. A., 2000: Deep geothermal drilling on the Reykjanes ridge opportunity for international collaboration. *Proceedings of the World Geothermal Congress 2000, Kyushu-Tohoku, Japan*, 3701-3706.

Fridleifsson, G.Ó., Albertsson, A., and Elders, W.A., 2010a: Iceland Deep Drilling Project (IDDP) – 10 years later – still an opportunity for international collaboration. *Proceedings of the World Geothermal Congress 2010, Bali, Indonesia,* 5 pp.

Fridleifsson, G.Ó., Albertsson, A., Elders, W., Sigurdsson, Ó., Karlsdóttir, R., Pálsson, B., 2011: The Iceland Deep Drilling Project (IDDP): planning for the second deep well at Reykjanes. Geothermal Resources Council, Transactions, 35, 347–354.

Fridleifsson, G.Ó, Albertsson, A., Pálsson, B., Stefánsson, B., Gunnlaugsson, E., Ketilsson, J., Lamarche, R., Andersen, P.E., 2010b: Iceland Deep Drilling Project. The first IDDP drill hole drilled and completed in 2009. *Proceedings of the World Geothermal Congress 2010, Bali, Indonesia*, 4 pp.

Fridleifsson, G.Ó., Pálsson, B., Albertsson, A.L., Stefánsson, B., Gunnlaugsson, E., Ketilsson, J., Gíslason, Th., 2015: IDDP-1 drilled into magma – world's first magma-EGS system created. *Proceedings World Geothermal Congress 2015, Melbourne, Australia*, 12 pp.

Fridleifsson, G.Ó., and Richter, B., 2010: The geological significance of two IDDP-ICDP spot cores from the Reykjanes geothermal field, Iceland. *Proceedings of the World Geothermal Congress 2010, Bali, Indonesia,* 6 pp.

Gercek, H., 2007: Poisson's ratio values for rocks. *Int. J. Rock Mech. & Mining Sciences, 44-1,* 1-13.

Guan Zhichuan and Chen Tinggen., 2016: *Drilling engineering theory and technology*. China University of Petroleum Press, Beijing, 263.

Guerra Guerrero, C.E.., 1998: Cementing of geothermal wells. Report 6 in: *Geothermal Training in Iceland,* UNU-GTP, Iceland, 157-188.

Halliburton., 2018: *Stage cementing tools.* Halliburton, website: *www.halliburton.com/en-US/ps/cementing/casing-equipment/stage-cementing-tools/default.page.*

Hernández R., Halliburton., and Bour D., 2010: Reverse-circulation method and durable cements provide effective well construction: a proven technology. *Proceedings of the 35th Workshop on Geothermal Reservoir Engineering, Stanford University, Stanford, CA,* 4 pp.

Hole, H.M., 2008a: Geothermal well cementing. In: *Petroleum Engineering Summer School, Dubrovnik, Croatia, Workshop, 26,* 6 pp, website: *www.geothermal-energy.org/pdf/IGAstandard/ISS/2008Croatia/Hole06.pdf.*

Hole, H.M., 2008b: Geothermal well design – casing and wellhead. In: *Petroleum Engineering Summer School, Dubrovnik, Croatia, Workshop, 26,* website: *www.geothermal-energy.org/pdf/IGAstandard/ISS/2008Croatia/Hole02.pdf*

Hólmgeirsson, S., Gudmundsson, Á., Pálsson, B., Bóasson, H.Á, Ingason K., and Thórhallsson, S., 2010: Drilling operations of the first Iceland Deep Drilling Well (IDDP). *Proceedings of the World Geothermal Congress 2010, Bali Indonesia,* 10 pp.

Huang Hefu, 2000: Study on deep geothermal drilling into a supercritical zone in Iceland. Report 7 in: *Geohtermal training in Iceland 2000.* UNU-GTP, Iceland, 105-137.

IGDCUG, 2014: *Overview of Tibet Yangbajing, Yangyi and Naqu hot fields*. Institute of geothermal development, China University of Geosciences (IGDCUG), website: *www.hbddrn.com*
Ingason, K., 2018: *Well designs and geothermal drilling technology*. UNU-GTP, Iceland, unpublished lecture notes.

Khaemba A., 2016: Drilling in Menengai high temperature field – drilling equipment and well design. *Presented at "SDG Short Course I on Exploration and Development of Geothermal Resources", organized by UNU-GTP, GDC and KenGen, Naivasha, Kenya*, 11 pp.

Liu Haiyang, 2014: *Analysis of temperature and pressure of well ZK212 in Yangyi geothermal field in Tibet, China.* University of Geosciences (Beijing), Beijing, 2002110030, 74 pp.

Nelson, E.B., 1990: *Well cementing*. Schlumberger Educational Services, Texas, 487 pp.

NZS, 2015*: Code of practice for deep geothermal wells, NZS 2403:2015*. Standards New Zealand, Wellington, NZ, 102 pp.

Thórhallsson, S., Pálsson, B., Hólmgeirsson, S., Ingason, K., Matthíasson, M., Bóasson, H.Á., and Sverrisson, H., 2010: Well design and drilling plans of the Iceland Deep Drilling Project (IDDP). *Proceedings of the World Geothermal Congress 2010, Bali, Indonesia*, 8 pp.

Wang Yanxin and Guo Qinghai, 2010: The Yangbajing geothermal field and the Yangyi geothermal field: two representative fields in Tibet, China. *Proceedings of the World Geothermal Congress 2010, Bali, Indonesia*, 5 pp.

Weisenberger T.B., Harðarson B.S., Kästner F., Gunnarsdóttir S.H., Tulinius H, Guðmundsdóttir V., Einarsson G.M., Pétursson F., Vilhjálmsson S., Stefánsson H.Ö., and Níelsson S., 2017: *Well report - RN-15/IDDP-2: Drilling in Reykjanes - phases 4 and 5 from 3000 to 4659 m.* ÍSOR – Iceland GeoSurvey, report ÍSOR-2017/053 (closed report), 276 pp.

APPENDIX I: Calculations on strength of casings

TABLE 1: Assessing axial loading before and during cementing

Grade	K55	C90	T95
Casing size (")	20	13 3/8	9 5/8
Casing size (mm)	508	339.73	244.48
LZ (m)	180	1500	3900
Wp (lb/ft)	133	80.7	61.1
Wp (kg/m)	197.9258	120.0948	90.92682
g (m / s^2)	9.81	9.81	9.81
ρif (kg/l)	1.85	1.8	1.6
Lif (m)	180	1500	3900
π	3.141593	3.141593	3.141593
d (mm)	475.7	310.3	212.7
D (mm)	508	339.7	244.5
ρef (kg/l)	1	1	1
Lef (m)	180	1500	3900
Fcsg air wt	349.5	1767.2	3478.8
Fcsg contents	564.9	2003.0	2175.1
Fdisplaced fluids	357.9	1333.6	1796.3
Fhooklood	556.5	2436.6	3857.6

TABLE 2: Tensile force during running and cementing casing

Grade	K55	C90	T95
Casing size (”)	20	13 3/8	9 5/8
Casing size (mm)	508.00	339.73	244.48
LZ (m)	180	1500	3900
Wp (lb/ft)	133	80.7	61.1
Fhooklood	556.5	2436.6	3857.6
pipe body strength (1000daN)	945	570	747
Pipe body strength (KN)	9450	5700	7470
Factor	17.0	2.3	1.9
Minimum design factor	1.8	1.8	1.8

TABLE 3: Fluid lifting force on anchor casing

Grade	C90
Casing size (”)	13 3/8
Casing size (mm)	339.73
Casing inside d (mm)	310.30
LZ (m)	1500
Wp (lb/ft)	80.7
Pw (MPa)	21.5
Fm (kN)	40.2
Fw (kN)	1585.7
Minimum tensile strength (kN)	5700
Calculation factor	3.6
Minimum design factor	1.8

TABLE 4: Thermal load on anchor casing (where applicable)

Grade	C90
Casing size (in)	13 3/8
Casing size (mm)	339.73
Casing inside d (mm)	310.30
Ea	0.000013
T1 (C)	123.00
T2 (C)	376.00
Ap (mm^2)	15014.68
Fc (kN)	-0.05
Fp (kN)	669.4
Fr	669.4
Pipe body strength (1000daN)	5700.00
Rising casing compressive strength (kN)	669.3
Design factor	8.5
Minimum Design factor	1.40

TABLE 5: Helical bucking due to self-weight plus thermal load (uncemented liner)

Grade	K55
Casing size (")	7
Casing size D (mm)	177.80
Casing inside d (mm)	143.80
Lz (m)	1200
Wp (lb/ft)	46
Wp (kg/m)	68.5
G	9.81
Ap (mm^2)	8587.6
D (mm)	177.80
E (mm)	38.1
Lp (mm^4)	28052650.7
Fc	97.3
Minimum yield stress (MPa)	379
Rj connection efficiency in compression	0.7
Total compressive stress fc (MPa)	97.3
Design factor	2.7
Minimum design factor	1

TABLE 6: Internal pressure at shoe during cementing

Grade	K55	C90	T95
Casing size (")	20	13 3/8	9 5/8
Casing size (mm)	508.00	339.73	244.48
W_p (lb/ft)	133	80.7	61.1
W_p (kg/m)	197.9	120.1	90.9
g (m/ s^2)	9.81	9.81	9.81
L_z (m)	180	1500	3900
ρ_c (kg/ l)	1.85	1.85	1.7
L_f (m)	180	1500	3900
ρ_f (kg/l)	1	1	1
$\triangle P_{internal}$ (MPa)	1.50	12.5	26.8
Internal yield pressure (MPa)	21.1	28.8	74.4
Calculated design factors	14.1	2.3	2.8
Design factors	1.5	1.5	1.5

TABLE 7: Wellhead internal pressure (shut-in steam/gas after drilling)

Grade	C90	T95
Nominal size (")	13 3/8	9 5/8
Nominal size (mm)	339.73	244.48
wellhead pressure (MPa)	21.5	21.5
Temperature saturation (°C)	371.791	371.791
Internal yield pressure	47.1	74.4
Ri	0.8	0.8
Design factor	1.8	2.8
Minimum design factor	1.8	1.8

TABLE 8: Wellhead internal pressure (shut-in steam/gas after drilling) where wellhead is fixed to the casing

Grade	**C90**
Nominal size (”)	13 3/8
Nominal size (mm)	339.73
Wellhead pressure (MPa)	21.5
D (mm)	339.73
d (mm)	310.3
ft (MPa)	253.5
Steel yield strength (MPa)	552
Design factor	2.2
Minimum design factor	1.5

TABLE 9: External pressure collapse (during cementing)

Grade	**K55**	**C90**	**T95**
Casing size (”)	20	13.375	9.625
Casing size (mm)	508	339.725	244.475
LZ (m)	200	1500	3900
ρc (kg/ l)	1.8	1.8	1.7
ρf (kg/ l)	1	1	1
$\triangle P_{external}$	1.4	11.8	26.8
Pipe collapse pressure (MPa)	10.3	25.4	67.6
Calculated design factors	7.3	2.2	2.5
Minimum design factor	1.2	1.2	1.2

TABLE 10: External pressure collapse (during production)

Grade	**C90**	**T95**
Casing size (”)	13.375	9.625
Casing size (mm)	339.725	244.475
Pressure wellhead (MPa)	21.5	21.5
Pressure casing shoe (MPa)	13.9	33.4
Difference external pressure (MPa)	13.9	33.4
Pipe collapse pressure (MPa)	25.4	67.6
Calculated design factors	1.8	2.0
Minimum design factor	1.2	1.2